Evaluating Spread Spectrum Techniques for Indoor LEO-PNT under Channel Impairments

Femke Wouters, Wout Van Uytsel, Thomas Janssen
Faculty of Applied Engineering, imec-IDLab, University of Antwerp, Antwerp, Belgium
{femke.wouters, wout.vanuytsel, thomas.janssen}@uantwerpen.be

***Abstract*—The rapid deployment of Low Earth Orbit (LEO) satellite constellations is transforming global connectivity, with potential applications extending beyond communication into precise Positioning, Navigation, and Timing (PNT). Their low altitude, high signal availability, and strong Doppler characteristics make LEO satellites a promising candidate for accurate and reliable localization, where traditional Global Navigation Satellite Systems (GNSS) fail. This study investigates the potential of LEO-based indoor positioning by comparing two spread spectrum techniques—Direct Sequence Spread Spectrum (DSSS) and Chirp Spread Spectrum (CSS)—in terms of resilience to Doppler shifts and multipath propagation in the acquisition stage. A MATLAB-based simulation framework was developed to mimic LEO signal conditions of an indoor environment. The results demonstrate that while DSSS offers strong Doppler resilience, its acquisition performance degrades under bandwidth constraints. In contrast, CSS maintains robust synchronization across varying channel impairments, preserving peak resolution even in severe multipath and spectrally constrained environments. The results indicate that CSS may offer advantages for next-generation LEO-based PNT applications, especially under challenging propagation conditions.**

***Index Terms*—CSS, DSSS, Indoor Positioning, LEO-PNT, Spread Spectrum**

I. Introduction

Accurate indoor localization has become increasingly important in recent years due to the growing demand for location-based services (LBS) in various domains such as asset tracking, healthcare monitoring, and emergency response systems. Despite the advancements in positioning technologies, achieving robust and reliable indoor localization remains a significant challenge due to the complex physical characteristics of such environments. While Global Navigation Satellite Systems (GNSS), including GPS and Galileo, have revolutionized outdoor navigation, their performance significantly diminishes in indoor environments due to signal blockage, attenuation, and multipath effects [1]. As alternatives, terrestrial-based positioning systems, such as Wi-Fi, Bluetooth, and Ultra-Wideband have been explored for indoor environments. Although these technologies can offer precise positioning [2], their accuracy and coverage are often constrained by infrastructure availability and scalability.

In recent years, Low Earth Orbit (LEO) satellites have emerged as a promising candidate to provide reliable positioning in both indoor and outdoor environments [3]. Due to their reduced orbital altitude (typically between 500 and 2,000 km), LEO satellites offer several advantages compared to Medium Earth Orbit (MEO) satellites used in traditional GNSS. LEO constellations often have more favorable geometric configurations for positioning, which lead to lower Geometric Dilution of Precision (GDOP) and consequently enhance positioning accuracy [4]. Moreover, the reduced transmission distance for LEO satellite signals results in significantly lower path loss, leading to stronger signal strength and improved signal penetration into indoor environments [3].

Nevertheless, there are several technical challenges to be addressed if the full potential of LEO satellites is to be realized for indoor positioning. These include significant Doppler shifts, frequent satellite handovers due to shorter visibility periods, signal attenuation, multipath effects, and near-far interference. In order to overcome these challenges, dedicated LEO-PNT (Positioning, Navigation and Timing) systems are being developed specifically for high-accuracy positioning and navigation purposes. Extensive research is being done in various segments, including the space, ground, and user segments, and signal design to optimize the performance of these emerging systems [5].

This study explores the extent to which signal processing, particularly spread spectrum techniques, can address key challenges in LEO-based indoor localization. These methods involve spreading the signal across a wider bandwidth to improve signal robustness and resistance to interference, effectively mitigating the effects of multipath propagation and signal degradation, which is particularly useful in indoor environments [6].

This paper compares the performance of two spread spectrum techniques—Direct Sequence Spread Spectrum (DSSS) and Chirp Spread Spectrum (CSS)—in the context of indoor localization using LEO-PNT signals. The objective is to address the following research question:

How do DSSS and CSS compare in terms of accuracy and resilience to Doppler shifts and multipath propagation in the acquisition of LEO-PNT-based indoor localization?

By evaluating these two spread spectrum techniques through both theoretical analysis and simulations, this study aims to explore their usability for indoor LEO-PNT. The remainder of this paper is structured as follows: Section II provides an overview of recent developments of spread spectrum methods for LEO-based positioning. This is followed by a description of the simulation methodology and signal models used to assess DSSS and CSS performance in Section III. The subse-

978-3-903176-77-5© 2025 IFIP

quent sections, Section IV and Section V, present the simulation results and their discussion, with a focus on Doppler shifts and multipath propagation effects. Finally, the paper concludes by summarizing the key findings and outlining avenues for future research in Section VI.

II. Related Work

LEO satellites are increasingly being explored as a promising solution for enhancing traditional GNSS for LBS. Three main approaches have emerged: using signals of opportunity from non-navigation satellites for positioning via Doppler or carrier-phase analysis [7]; augmenting GNSS with correction data or relayed signals to improve performance in difficult environments [8]; and deploying dedicated LEO-PNT constellations with purpose-built signals and payloads for high-precision global coverage [5]. This paper focuses on the third approach, evaluating its potential for reliable indoor localization. A review of the current literature on signal design for dedicated LEO-PNT systems reveals that the use of other spread spectrum techniques than Direct Sequence Spread Spectrum (DSSS) remains an underexplored area. In this section, three key techniques are examined—DSSS, Frequency Hopping Spread Spectrum (FHSS), and Chirp Spread Spectrum (CSS)—highlighting their advantages and potential applicability within LEO-PNT architectures for indoor positioning.

1) Direct Sequence Spread Spectrum: DSSS has been widely employed in communication and navigation systems, including GNSS, 3G cellular networks, and IEEE 802.11b Wi-Fi, and serves as the core spreading method in Code Division Multiple Access (CDMA) systems [9]. By modulating data with a high-rate pseudorandom sequence, DSSS spreads the signal across a wide bandwidth, lowering its power spectral density and enhancing resilience against interference, jamming, and interception. In the context of indoor localization, DSSS offers several advantages. The despreading process at the receiver concentrates the signal energy while distributing noise and interference, thereby improving the signal-to-noise ratio (SNR) and mitigating multipath propagation [10].

Nevertheless, its susceptibility to the near-far problem, where stronger interfering signals can overwhelm weaker ones, remains a limitation [11]. Moreover, studies show that the significant Doppler shifts of LEO satellites introduce additional challenges in achieving precise carrier and code phase synchronization. These shifts expand the acquisition search space, increasing both signal acquisition time and computational complexity [12]. In order to address this, alternative signal acquisition methods have been proposed. FFT-based techniques continue to serve as a foundational approach, with enhancements such as approximate kernel functions [13] and hierarchical search strategies [14] that aim to reduce processing overhead while maintaining detection performance. Given its successful deployment in navigation systems and its capacity to enhance robustness in multipath-dense environments, DSSS was included in this study as a baseline technique for evaluating spread spectrum performance in LEO-PNT-based indoor localization.

2) Frequency Hopping Spread Spectrum: FHSS has received comparatively less attention in satellite-based positioning than DSSS, despite its long history in secure communications and its wide use in wireless technologies such as Bluetooth [6]. By rapidly switching the carrier frequency according to a pseudorandom sequence shared between transmitter and receiver, FHSS offers strong resilience against interference, jamming, and the near-far problem, as no single frequency is occupied long enough to be consistently disrupted [6]. Recent studies by Jung et al. [15] and Prasetyo Adi et al. [16] demonstrate that FHSS-based systems can significantly improve interference resilience and data reliability in dynamic LEO environments. Although the primary focus of this research is on satellite communication rather than positioning, the findings underscore the potential of FHSS for achieving robust signal performance in such environments. However, further research is required to assess its suitability for accurate and resilient positioning in LEO-PNT systems. Given these gaps and the focus of this paper, FHSS was not considered in this work.

3) Chirp Spread Spectrum: CSS has recently emerged as a promising candidate for LEO-PNT systems due to its inherent resilience to interference, multipath propagation, and Doppler effects [17]. Utilizing linear frequency modulation—commonly referred to as chirping—CSS has been successfully deployed in long-range, low-power communication systems such as LoRa. Its potential is increasingly being explored in the field of satellite communications. One of CSS's key advantages is its low acquisition complexity due to its less stringent synchronization requirements. Egea-Roca et al. [12] have shown that CSS can reduce acquisition complexity by up to two orders of magnitude compared to DSSS. Additionally, CSS's continuous chirp structure allows for effective Doppler shift tracking and compensation [18]. Recent research has further refined CSS signal design specifically for LEO-PNT purposes by introducing pilot/data structures, hybrid modulation schemes, and optimized chirp parameters, improving sensitivity, ranging accuracy, and data throughput [19], [20]. Despite its strengths, CSS faces scalability challenges in high-user-density scenarios due to inter-signal interference stemming from imperfect orthogonality [12]. In order to address this, recent studies proposed enhancements such as fractional chirp rate designs (FCR-CSS) [21] and advanced waveform structures like Symmetry CSS (SCSS) [22] and Asymmetry CSS (ACSS) [23], improving both correlation performance and system capacity.

Although research has demonstrated the benefits of CSS for LEO-PNT, a comparative study between CSS and other spread spectrum techniques, particularly DSSS, in terms of their performance in indoor localization remains sparse. This gap presents an opportunity to investigate the performance of CSS relative to DSSS, specifically within indoor LEO-PNT applications. In this work, we take a first step toward analyzing their performance through experiments.

III. Methodology

This section outlines the simulation framework developed to evaluate and compare the performance of two spread spectrum techniques—DSSS and CSS—under LEO-PNT-like conditions. It includes the signal models for both techniques, along with environmental configurations representing a LEO satellite constellation and an indoor propagation environment. The signals are subjected to environmental effects such as Doppler shift and multipath propagation, after which the performance of each technique is assessed in terms of signal acquisition and robustness. The simulation environment was implemented in MATLAB.

A. Signal Modeling

This part of the simulation framework models both DSSS and CSS signals and upconverts them to a carrier frequency of $1575.42\,\text{MHz}$, corresponding to the GPS L1 band [1]. The sampling frequency is set to $10\,\text{MHz}$. In order to ensure a fair comparison, both DSSS and CSS signals are allocated a spread bandwidth of $2.046\,\text{MHz}$.

1) DSSS: The DSSS signal is constructed using a pseudorandom noise (PRN) sequence with a sequence length of $1023\,\text{chips}$ and a chip rate (R_c) of $1.023\,\text{Mbps}$, which is directly proportional to the spread bandwidth. These values have been chosen to align with the GPS L1 standard, providing a meaningful baseline for comparison. Following the spreading process, the baseband signal is modulated using Binary Phase Shift Keying (BPSK). Fig. 1 shows an example of the DSSS spreading process, along with the resulting BPSK-modulated signal.

At the receiver, the acquisition of the DSSS signal involves estimating the Doppler shift (f_d) and code delay (τ_{chip}), which arise due to the relative motion between the satellite and receiver, and the signal propagation time, respectively. In order to improve computational efficiency over traditional two-dimensional search methods, an FFT-based correlation approach is employed. This method involves computing the correlation $R(\tau_{chip}, f_d)$ between the received signal and a locally generated PRN sequence, across a range of Doppler frequencies [6]. As defined in (1), the estimated Doppler shift ($\hat{f}_d$) is determined by identifying the frequency that yields the maximum correlation across all delays.

$$\hat{f}_d = \arg\max_{f_d} \max_{\tau_{chip}} |R(\tau_{chip}, f_d)| \tag{1}$$

Once $\hat{f}_d$ is identified, the code delay $\hat{\tau}_{chip}$ is estimated by locating the earliest delay that maximizes the correlation or reaches the minimum threshold at this frequency, as shown in (2).

$$\hat{\tau}_{chip} = \arg\max_{\tau_{chip}} \left| R(\tau_{chip}, \hat{f}_d) \right| \tag{2}$$

2) CSS: The CSS signal is generated using Binary Offset Keying (BOK), where each data bit is represented by either an up-chirp or a down-chirp. This modulation scheme was selected for its simplicity, as it offers a straightforward and efficient way to map binary data to frequency shifts [19].

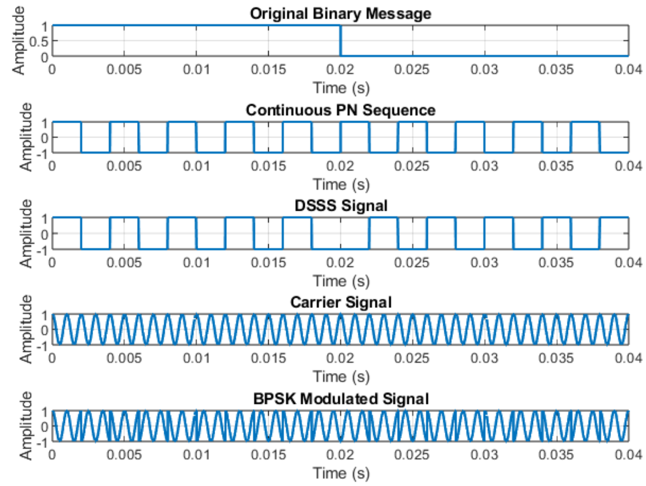

Fig. 1: Example of DSSS signal construction using a binary message [1 0] and a pseudorandom sequence [1010101010]. The subplots show: (1) input data, (2) PRN sequence, (3) spread baseband signal (1 kHz bandwidth), (4) carrier signal (1 kHz), and (5) BPSK-modulated output.

The up-chirp increases in frequency over time, while the down-chirp decreases, with each chirp sweeping over the $2.046\,\text{MHz}$ bandwidth over a duration of $50\,\text{ms}$, yielding a linear chirp rate (μ) of approximately $40.92\,\text{MHz/s}$. Fig. 2 illustrates an example of BOK-CSS signal generation using the binary sequence [1 0], where the waveform is composed of an up-chirp followed by a down-chirp. The configuration parameters used in this study are based on the design recommendations presented in the study by Egea-Roca et al. [12], which proposes optimized multi-satellite access schemes and signal configurations, including chirp durations tailored for constellations of 50 and 100 LEO satellites.

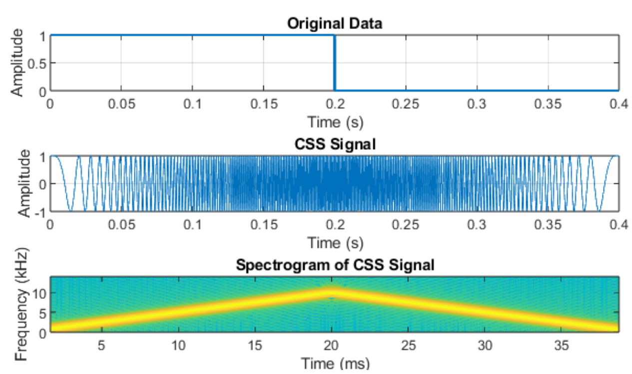

Fig. 2: Example of BOK-CSS signal generation using the binary sequence [1 0], with a bandwidth of $1\,\text{kHz}$, a carrier frequency of $0\,\text{Hz}$, and a chirp duration of $0.2\,\text{s}$. Subplots show: (1) input data, (2) corresponding BOK-CSS signal, and (3) spectrogram.

In order to enable accurate acquisition and synchronization of the CSS signal at the receiver, a dedicated synchronization signal is transmitted in the first time slot, prior to the data-bearing chirps. This synchronization signal consists of a coherent sum of an up-chirp and a down-chirp, as shown in Fig. 3. The estimation process involves dechirping the received synchronization signal with both chirp types, followed by FFT-based spectral analysis. The resulting frequency content of the dechirped signals reveals spectral peaks corresponding to delay- and Doppler-induced frequency shifts [12]. As demonstrated in (3), the estimated delay ($\hat{\tau}$) is computed as the frequency difference between the dechirped up- and down-chirps.

$$\hat{\tau} = \frac{f_{\text{up}} - f_{\text{down}}}{2 \cdot \mu} \tag{3}$$

where f_{up} and f_{down} are the peak frequencies in the up- and down-chirp FFT spectra, respectively, and μ is the chirp rate. The Doppler shift ($\hat{f}_d$) is estimated by computing the average of these frequencies, as shown in (4).

$$\hat{f}_d = \frac{f_{\text{up}} + f_{\text{down}}}{2} \tag{4}$$

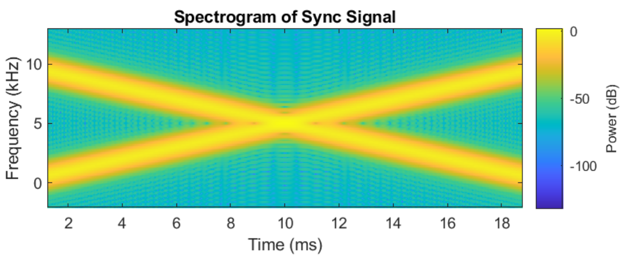

Fig. 3: Time-frequency representation of an example synchronization signal, with a bandwidth of $1\,\text{kHz}$, a carrier frequency of $0\,\text{Hz}$, and a chirp duration of $0.2\,\text{s}$.

B. Environment Simulation

In order to evaluate the performance of satellite-based positioning under varying conditions, the simulation environment consists of two key components: a LEO satellite constellation and an indoor propagation model.

The simulation of the LEO satellite constellation is constructed based on the orbital parameters typical of LEO satellites, such as altitude, velocity, orbital inclination, coverage area, and orbital period. Due to the absence of official LEO-PNT system specifications, the constellation model for this study is founded upon the paper by Çelikbilek et al. [24], which provides a methodology for designing LEO constellations tailored to PNT applications. In order to model the satellite constellation, we used MATLAB's Satellite Communication Toolbox.

Within this framework, the constellation itself consists of three orbital shells. The first shell is a Walker Star constellation 133/19/1 at an altitude of 1835 km with an inclination of 34 °. The second shell is a Walker Delta 99/3/1 at an altitude of 1550 km with an inclination of 86 °. The third shell a Walker Delta 150/30/1 at an altitude of 1477 km with an orbital inclination of 80 °.

In addition to the satellite constellation, the indoor environment is a factor affecting signal performance due to phenomena such as attenuation, multipath propagation, signal blockage, and interference. We model the attenuation by reducing the amplitude of the signal relative to the nominal value.

C. Simulation of Observables

This study focuses on two key factors that affect the performance of LEO-PNT systems: the Doppler effect and multipath propagation. Both of these phenomena can significantly degrade signal quality and reduce positioning accuracy.

In order to provide a more realistic signal reception model, a propagation time delay is introduced. This delay, denoted by τ, corresponds to the time required for the signal to cover the distance d between the satellite and ground-based receiver [17], as expressed by (5).

$$\tau = \frac{d}{c} \tag{5}$$

where c is the speed of light in a vacuum. In practical terms, this delay is simulated by inserting a sequence of zeros, equivalent to the time of τ, at the beginning of the transmitted signal for both DSSS and CSS modulation schemes. This approach effectively shifts the signal in time without modifying its inherent structure. It is important to note that the perception of time delay differs between DSSS and CSS due to their distinct signal structures. CSS employs long-duration chirps, resulting in a delay perception that encompasses the full frame length rather than being confined to a single symbol. In contrast, DSSS relies on PRN codes of fixed length, limiting the delay range that one is able to recover without the use of data to one PRN sequence.

Complementing the delay model is the simulation of the Doppler shift, which manifests as a frequency offset in the received signal. This shift arises from the relative motion between the transmitter (satellite) and the receiver (ground station), with the magnitude of the shift determined by their instantaneous relative velocity v_{rel} along the line of sight (LOS) path. This Doppler shift is computed according to (6).

$$f_d = \frac{v_{\text{rel}}}{c} \cdot f_c \tag{6}$$

Here, f_d is the Doppler shift, c is the speed of light, and f_c is the carrier frequency of the transmitted signal [17]. In this study, the simulation dynamically computes f_d at each time step to adjust the signal frequency accordingly, ensuring realistic modeling of Doppler-induced frequency offsets. For signals operating in the GPS L1 band, typical Doppler shifts for LEO satellites range approximately from $-35\,\text{kHz}$ to $+35\,\text{kHz}$, depending on orbital parameters and elevation angles [12].

In addition to delay and frequency effects, multipath propagation represents another significant challenge in LEO-PNT signal integrity. This phenomenon occurs when a transmitted signal reaches the receiver via multiple paths, caused by reflections off surfaces such as buildings or other obstructions.

TABLE I: Simulation scenarios for DSSS and CSS evaluation

Signal	Scenario	Delay [samples]	Doppler shift [Hz]	Multipath components
DSSS	DSSS-D1	2,000	+20,000	/
DSSS	DSSS-D2	8,000	+20,000	/
DSSS	DSSS-MP	2,000	+20,000	Path 1: +50 samples, attenuation 1.5 Path 2: +2,000 samples, attenuation 0.7
CSS	CSS-D1	100,000	+20,000	/
CSS	CSS-MP	100,000	+20,000	Path 1: +50 samples, attenuation 1.5 Path 2: +20,000 samples, attenuation 0.7

These multiple signal paths result in delayed and attenuated replicas of the original signal, leading to signal distortion and potentially degrading positioning accuracy. In the simulation, multipath is modeled in a simplified way. Each multipath signal is modeled by introducing a specific time delay τ_i and an associated attenuation factor α_i, where i indexes each multipath path. The resulting received signal $r(t)$ is given by (7).

$$r(t) = \sum_{i=0}^{N} \alpha_i \cdot s(t - \tau_i) \tag{7}$$

Here, $s(t)$ is the original transmitted signal and N denotes the total number of multipath components, with $i = 0$ corresponding to the direct LOS path [17]. This model enables analysis of multipath-induced signal distortion and its impact on acquisition performance.

D. Performance Evaluation

In order to evaluate the impact of Doppler shift and multipath propagation on the performance of DSSS and CSS, a series of test scenarios were defined and implemented within the simulation framework. Each scenario models a different combination of propagation effects, as shown in Table I, to assess signal robustness and acquisition performance under varying levels of channel effects. In addition to these scenarios, several additional configurations were tested to explore a broader range of channel conditions.

For DSSS, three scenarios were implemented to isolate the effects of propagation impairments:

- **DSSS-D1:** A moderate-delay, high-Doppler scenario.
- **DSSS-D2:** A high-delay, high-Doppler scenario.
- **DSSS-MP:** A multipath scenario that builds on DSSS-D1 by introducing two delayed and attenuated replicas of the original signal.

In parallel, for CSS, two scenarios were constructed to evaluate performance under comparable conditions:

- **CSS-D1:** A high-delay, high-Doppler scenario.
- **CSS-MP:** A multipath scenario that builds on CSS-D1 by introducing two delayed and attenuated replicas of the original signal.

IV. Results

This section presents the performance evaluation of DSSS and CSS signal estimation under varying channel conditions, including time delay, Doppler shift, and multipath propagation.

A. Doppler Effect & Time Delay

The performance of DSSS signal estimation was evaluated under two scenarios, referred to as DSSS-D1 and DSSS-D2. In the first scenario, DSSS-D1, which includes a moderate time delay and high Doppler shifts, the correlation surface showed a sharp and well-defined peak with a maximum value of 250. In contrast, scenario DSSS-D2, characterized by a significantly larger time delay, produced a broader correlation peak with a reduced maximum value of 16. As shown in Fig. 4a and Fig. 4b, these results highlight the robustness of DSSS under moderate propagation conditions, while larger delays lead to a notable degradation in performance due to the zero's added before the signal.

The evaluation of the CSS signal was conducted under scenario CSS-D1, which combines large time delays with high Doppler shifts. The results indicate that CSS maintains high estimation accuracy under these conditions, consistently providing precise time delay and Doppler shift estimates. Further testing confirmed that the system's performance remains resilient to variations in time delay as well as to Doppler shifts of varying magnitudes and directions. As shown in Fig. 5a, the FFT spectra of the dechirped synchronization signal demonstrate well-defined, symmetric spectral peaks, enabling accurate and easy parameter estimation.

B. Multipath Propagation

The effect of multipath propagation on DSSS signal estimation was evaluated under the DSSS-MP scenario. As shown in Fig. 4c, multiple correlation peaks were observed, corresponding to both the LOS path and the multipath components. Fig. 4d also shows a zoomed-in view to demonstrate that even when a multipath component arrives with a minimal delay relative to the LOS signal, two distinct correlation peaks can still be identified. It is also important to note that the first multipath component exhibited stronger attenuation than the LOS signal. Despite this, the system is still able to estimate the code delay and Doppler shift for the LOS signal, as the correlation peak remains sharp and identifiable. However, when the spread bandwidth is reduced by a factor of ten, the resulting correlation function becomes significantly degraded, as shown in Fig. 4e. In this case, the correlation peak appears wider and more distorted, reducing the system's ability to accurately estimate the code delay of the LOS signal.

Similarly, the effect of multipath on CSS signal estimation was evaluated in the CSS-MP scenario. As shown in

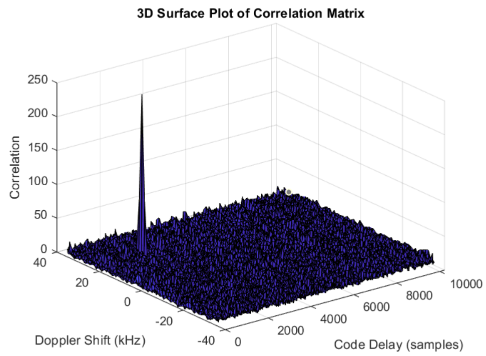

(a) DSSS-D1: Sharp peak (max=250)

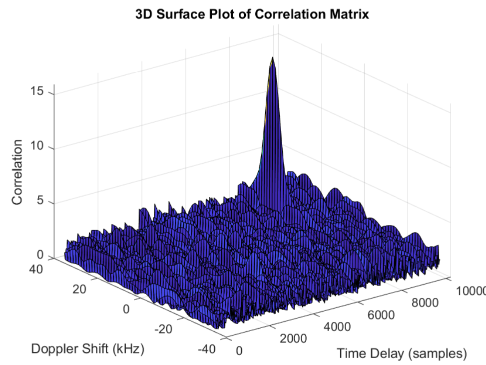

(b) DSSS-D2: Broader peak (max=16)

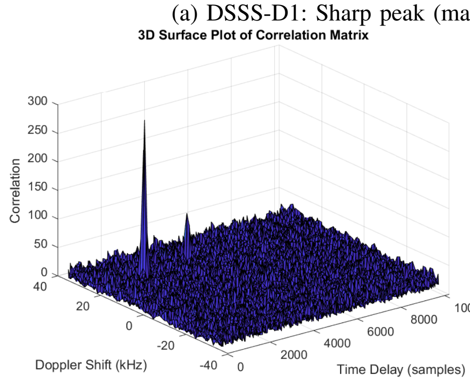

(c) DSSS-MP

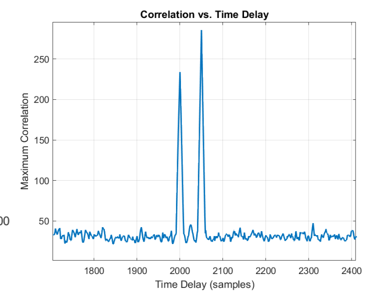

(d) DSSS-MP (zoomed delay peak)

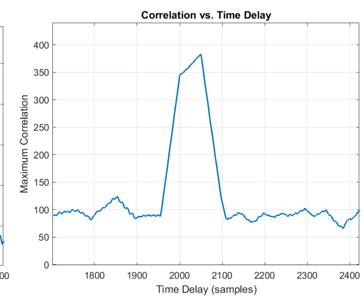

(e) DSSS-MP (lower BW)

Fig. 4: Correlation search spaces showing the impact of time delay, Doppler shift (a),(b), and multipath propagation (c),(d),(e) on DSSS signal acquisition.

Fig. 5b, multiple spectral peaks appear in the FFT plots of the dechirped up- and down-chirp signals, corresponding to the LOS path and the multipath components. A zoomed-in view of the down-chirp peak, as shown in Fig. 5c, reveals that even when a multipath component arrives with a delay close to the LOS signal, two distinct peaks remain visible in the spectral domain. When the spread bandwidth is reduced by a factor of ten, the resulting spectrum, shown in Fig. 5d, exhibits a slightly distorted correlation peak. However, both the LOS and multipath peaks remain distinguishable.

V. Discussion

A. DSSS

The simulation results provide valuable insights into the acquisition performance of DSSS signals in LEO-PNT environments. Our findings show that the DSSS system exhibits strong resilience to variations in Doppler shift, irrespective of the magnitude and direction. However, the larger Doppler shifts in LEO environments significantly expand the Doppler search space, increasing computational load.

Furthermore, in scenarios involving moderate time delay, the autocorrelation properties of the PRN sequence produce sharp correlation peaks for both delay and Doppler shift, reflecting accurate temporal alignment. However, as the time delay increases, particularly when the delay becomes comparable to the frame length of the signal, the correlation structure deteriorates. This degradation arises from the finite-length transmission model of DSSS, where the signal is transmitted in discrete frames. When the delay causes misalignment beyond the frame boundaries, fewer PRN chips overlap between the received signal and the locally generated reference, resulting in broader, lower-amplitude correlation peaks. Consequently, the estimation uncertainty increases, reducing the accuracy of delay and Doppler shift estimation. In order to address this, a continuous transmission model similar to that used in GPS systems should be adopted [1]. In such a model, the signal repeats indefinitely, so any time delay manifests as a cyclic code phase shift rather than an absolute offset, preserving correlation properties and enabling more robust synchronization under large delays. We identify this as one of the limitations of this study, and future work could incorporate this wrap-around to mimic GNSS signals more realistically.

The impact of multipath propagation further highlights the strengths and limitations of the DSSS approach. In a multipath environment, each propagation path gives rise to a distinct peak in the correlation plot, with its position and amplitude determined by its respective delay and attenuation. The results show that even in scenarios where a multipath component arrives with minimal delay relative to the LOS signal, the DSSS system is capable of resolving two distinct correlation peaks. This is due to the high time resolution afforded by the wide spread bandwidth. Nevertheless, when

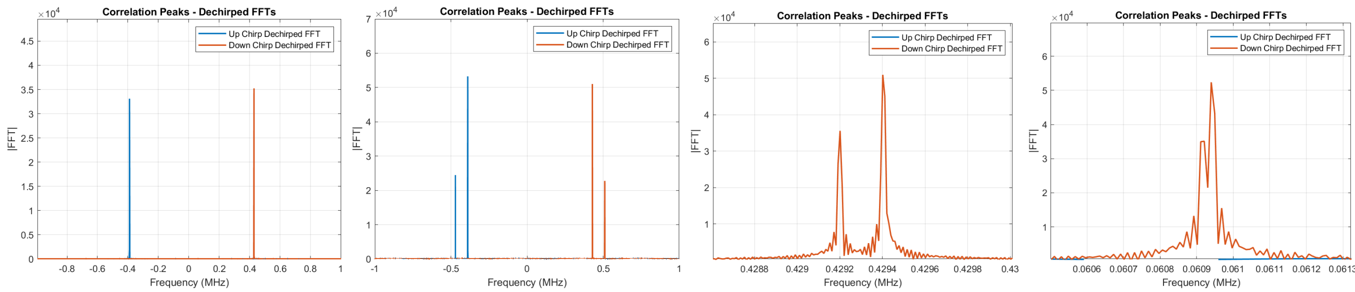

(a) CSS-D1 (b) CSS-MP (c) CSS-MP (zoomed-in) (d) CSS-MP (lower BW)

Fig. 5: FFT spectra showing the impact of time delay, Doppler shift (a) and multipath propagation (b),(c),(d) on CSS signal acquisition.

the spread bandwidth is reduced by a factor of ten, the resulting correlation peak becomes broadened and distorted, impairing the system's ability to isolate the LOS signal in the acquisition step. These findings underscore the role of spread bandwidth in determining acquisition performance. A higher spread bandwidth allows for faster PRN sequences, which improves resilience to multipath interference, but at the cost of increased bandwidth.

B. CSS

The simulation results for CSS demonstrate its robustness and accuracy under challenging channel conditions, including large time delays, high Doppler shifts, and multipath. This performance advantage stems from the fundamental signal structure of CSS. Unlike conventional correlation-based synchronization techniques, which may exhibit performance degradation as delay or Doppler increases, the CSS approach consistently maintains spectral integrity, resulting in sharp and well-defined correlation peaks. Moreover, the results demonstrate that CSS synchronization is highly resilient to multipath propagation. Despite the presence of multiple paths, including cases where a multipath component had a greater amplitude than the LOS signal, the algorithm consistently retrieved the correct parameters.

One of the primary reasons for this robustness lies in the use of a dual-chirp synchronization signal, consisting of up- and down-chirps, enabling efficient separation of the time delay and Doppler effect through a frequency-domain approach. During the acquisition of the synchronization signal, the dechirping process transforms the time delays into frequency shifts, while the Doppler shifts manifest as symmetric offsets around the central frequency. This results in clear, symmetric spectral peaks, allowing for independent, accurate estimation of each parameter via relatively simple algebraic computations. By representing delays as frequency components, CSS maintains its correlation structure even in the presence of large delays, thereby ensuring reliable synchronization under challenging propagation conditions.

Importantly, the findings also highlight that when the spread bandwidth is reduced by a factor of ten, a scenario that significantly degrades DSSS performance, the CSS system continues to distinguish between the LOS and multipath components in the acquisition stage. Although the spectral peaks are broadened and exhibit a slight distortion under reduced bandwidth, they remain individually identifiable. This enhanced separability is attributed to the Frequency-Modulated Continuous Wave (FMCW) nature of CSS signals. The linear chirp structure induces a direct mapping between time delays and frequency shifts upon dechirping, enabling fine-grained resolution in the frequency domain. Consequently, closely spaced multipath components that are challenging to separate using conventional time-domain correlation methods can still be resolved as distinct spectral peaks. This inherent property of chirp-based signaling provides CSS with superior resolution capabilities, particularly in bandwidth-constrained environments.

VI. Conclusion

This study evaluated the acquisition performance of DSSS and CSS signals within LEO-PNT environments, particularly under challenging conditions, such as large Doppler shifts and multipath propagation. While DSSS provides robust performance against Doppler shifts, it increases the computational complexity of acquisition significantly. This spread spectrum technique experiences limitations under reduced bandwidth, which impair its multipath resolution capabilities in the acquisition stage. Moreover, for DSSS to function effectively under large time delays, a continuous transmission model is essential to preserve code phase coherence and enable accurate acquisition and tracking, which we identify as a limitation of this study. In contrast, CSS consistently delivers higher acquisition accuracy and robustness in challenging LEO-PNT environments characterized by significant Doppler shifts and multipath. Overall, while DSSS remains a viable solution, CSS's enhanced acquisition speed, precision, and robustness make it a promising candidate for reliable localization using LEO satellite signals, especially in spectrally limited and complex propagation environments.

Building on these findings, future research should extend the current simulation framework to incorporate a broader spectrum of realistic conditions, including the near-far problem, co-channel interference, and hardware impairments. Additionally, refining the indoor environment model and overall propagation models to capture signal transitions from space through the atmosphere into indoor settings will provide a more comprehensive understanding of LEO signal behavior. Since the current study is focused primarily on modeling Doppler shift and multipath rather than attenuation, a full link budget analysis remains a key area for future work to evaluate signal performance in complex indoor settings. The present study focuses on the acquisition process, while the implementation of a tracking stage is left for future work to enable a more complete performance assessment. Moreover, further exploration of other spread spectrum techniques, such as FHSS, as a complementary or alternative approach, may reveal new opportunities for enhancing the reliability and accuracy of indoor LEO-PNT systems.

In conclusion, this study establishes a foundational understanding of the trade-offs between DSSS and CSS in terms of acquisition, highlighting the strengths and limitations of each technique under indoor propagation conditions. As the demand for high-precision indoor localization continues to grow, future advancements in LEO-PNT systems will depend on the integration of advanced and resilient signal processing strategies capable of mitigating these impairments and ensuring reliable, high-accuracy performance in complex environments.

References

[1] F. Van Diggelen, *A-gps: Assisted gps, gnss, and sbas*. Artech house, 2009.

[2] T. Janssen, A. Koppert, R. Berkvens, and M. Weyn, "A Survey on IoT Positioning Leveraging LPWAN, GNSS, and LEO-PNT," *IEEE Internet of Things Journal*, vol. 10, no. 13, pp. 11 135–11 159, Jul. 2023.

[3] R. M. Ferre, E. S. Lohan, H. Kuusniemi, J. Praks, S. Kaasalainen, C. Pinell, and M. Elsanhoury, "Is LEO-based positioning with mega-constellations the answer for future equal access localization?" *IEEE Communications Magazine*, vol. 60, no. 6, pp. 40–46, 2022.

[4] F. S. Prol, S. Kaasalainen, E. S. Lohan, M. Z. H. Bhuiyan, J. Praks, and H. Kuusniemi, "Simulations using LEO-PNT systems: A Brief Survey," in *2023 IEEE/ION Position, Location and Navigation Symposium (PLANS)*, Apr. 2023, pp. 381–387.

[5] F. S. Prol, M. Z. H. Bhuiyan, S. Kaasalainen, E. S. Lohan, J. Praks, K. Çelikbilek, and H. Kuusniemi, "Simulations of Dedicated LEO-PNT Systems for Precise Point Positioning: Methodology, Parameter Analysis, and Accuracy Evaluation," *IEEE Transactions on Aerospace and Electronic Systems*, vol. 60, no. 5, pp. 6499–6516, Oct. 2024.

[6] J. K. Holmes, *Spread spectrum systems for GNSS and wireless communications*. Artech House Norwood, 2007.

[7] W. Stock, R. T. Schwarz, C. A. Hofmann, and A. Knopp, "Survey On Opportunistic PNT With Signals From LEO Communication Satellites," *IEEE Communications Surveys & Tutorials*, pp. 1–1, 2024.

[8] Y. Meng, L. Bian, L. Han, W. Lei, T. Yan, M. He, and X. Li, "A Global Navigation Augmentation System Based on LEO Communication Constellation," in *2018 European Navigation Conference (ENC)*, May 2018, pp. 65–71.

[9] K. Wong and T. O'Farrell, "Spread spectrum techniques for indoor wireless IR communications," *IEEE Wireless Communications*, vol. 10, no. 2, pp. 54–63, Apr. 2003.

[10] P. Flikkema, "Spread-spectrum techniques for wireless communication," *IEEE Signal Processing Magazine*, vol. 14, no. 3, pp. 26–36, May 1997.

[11] D. Magill, F. Natali, and G. Edwards, "Spread-spectrum technology for commercial applications," *Proceedings of the IEEE*, vol. 82, no. 4, pp. 572–584, Apr. 1994.

[12] D. Egea-Roca, J. A. López-Salcedo, G. Seco-Granados, and E. Falletti, "Comparison of several signal designs based on chirp spread spectrum (CSS) modulation for a LEO PNT system," in *Proceedings of the 34th International Technical Meeting of the Satellite Division of The Institute of Navigation (ION GNSS+ 2021)*, 2021, pp. 2804–2818.

[13] S. Zhang, G. Wan, S. Wang, X. Li, X. Zhang, and C. Shi, "A Fast DSSS Signal Acquisition Method with Low Computing Load Based on Approximate Kernel FFT/IFFT," in *2023 3rd Asia-Pacific Conference on Communications Technology and Computer Science (ACCTCS)*, Feb. 2023, pp. 319–323.

[14] M. He, Y. He, Y. Shen, and Z. Ma, "Fast Signal Acquisition Algorithm Based on Doppler Frequency Hierarchical Search Strategy," in *2024 4th International Conference on Electronics, Circuits and Information Engineering (ECIE)*, May 2024, pp. 422–428.

[15] S. Jung, S. Jeong, J. Kang, G. Im, S. Lee, M.-K. Oh, J. G. Ryu, and J. Kang, "LR-FHSS Transceiver for Direct-to-Satellite IoT Communications: Design, Implementation, and Verification," Mar. 2024.

[16] P. D. Prasetyo Adi, E. Dogheche, I. Dayoub, K. Stekelorom, D. Remiens, and N. Armi, "Improvement of LR-FHSS LPWAN Satellite Communication for IoMT," in *2024 7th International Seminar on Research of Information Technology and Intelligent Systems (ISRITI)*, Dec. 2024, pp. 126–131, iSSN: 2832-1456.

[17] B. Sklar, *Digital communications: fundamentals and applications*. Pearson, 2021.

[18] A. Gabbrielli, G. K. J. Fischer, T. Schaechtle, W. Xiong, D. J. Schott, J. Bordoy, J. Wendeberg, F. Höflinger, C. Schindelhauer, and S. J. Rupitsch, "Airborne Acoustic Chirp Spread Spectrum Communication System for User Identification in Indoor Localization," *IEEE Transactions on Instrumentation and Measurement*, vol. 72, pp. 1–15, 2023.

[19] D. Egea-Roca, J. A. López-Salcedo, and G. Seco-Granados, "Performance Analysis of the Pilot and Data Component of a CSS Signal for LEO-PNT," *Engineering Proceedings*, vol. 54, no. 1, p. 35, 2023.

[20] D. Egea-Roca, J. Lopez-Salcedo, G. Seco-Granados, and E. Falletti, "Performance analysis of a multi-slope chirp spread spectrum signal for PNT in a LEO constellation," in *2022 10th Workshop on Satellite Navigation Technology (NAVITEC)*. IEEE, 2022, pp. 1–9.

[21] R. Zhang, S. Zhang, and J. Ma, "Fractional Chirp Rate Based CSS Multiple Access for LEO Satellite: Design and Implementation," in *2024 IEEE/CIC International Conference on Communications in China (ICCC)*, Aug. 2024, pp. 746–751.

[22] Y. Qian, L. Ma, and X. Liang, "Symmetry Chirp Spread Spectrum Modulation Used in LEO Satellite Internet of Things," *IEEE Communications Letters*, vol. 22, no. 11, pp. 2230–2233, Nov. 2018.

[23] ——, "The Performance of Chirp Signal Used in LEO Satellite Internet of Things," *IEEE Communications Letters*, vol. 23, no. 8, pp. 1319–1322, Aug. 2019.

[24] K. Çelikbilek, E. Simona Lohan, and J. Praks, "Optimization of a LEO-PNT Constellation: Design Considerations and Open Challenges," *International Journal of Satellite Communications and Networking*, 2025.